

The non-commutivity of shear wave splitting operators at low frequencies and implications for anisotropy tomography

Paul G. Silver^{1,*} and Maureen D. Long²

¹Department of Terrestrial Magnetism, Carnegie Institution of Washington, 5241 Broad Branch Road, NW, Washington, DC 20015, USA

²Department of Geology and Geophysics, Yale University, P.O. Box 208109, New Haven, CT 06520, USA. E-mail: maureen.long@yale.edu

Accepted 2010 December 20. Received 2010 December 11; in original form 2010 May 14

SUMMARY

Measurements of the splitting or birefringence of seismic shear waves constitute a powerful and popular technique for characterizing azimuthal anisotropy in the upper mantle. The increasing availability of data sets from dense broad-band seismic arrays has driven interest in the development of techniques for the tomographic inversion of shear wave splitting data and in comparing splitting measurements with anisotropic upper-mantle models obtained from other constraints, such as surface wave analysis. Two different theoretical approaches have been developed for predicting apparent shear wave splitting parameters (fast direction and delay time) for models that include multiple layers of anisotropy at depth, which is useful for comparing azimuthally anisotropic surface wave models with shear wave splitting measurements. These approaches differ in one key aspect, which is whether or not the shear wave splitting operator can be treated as commutative. In this paper, we investigate the theoretical source of this discrepancy, and show that at frequencies relevant to most studies of upper-mantle anisotropy, the term that results in the non-commutivity of the shear wave splitting operator in the expressions for multiple-layer splitting must be retained. In contrast, the quantity known as the splitting intensity, which is closely related to the apparent fast direction and delay time, does commute at these frequencies. We illustrate these inferences with forward modelling examples and discuss their implications for the tomographic inversion of shear wave splitting measurements, the comparison of surface wave models with shear wave splitting observations and the joint inversion of surface wave and shear wave splitting observations for upper-mantle anisotropic models.

Key words: Seismic anisotropy; Seismic tomography; Wave propagation.

1 INTRODUCTION

The characterization of seismic anisotropy in the Earth's upper-mantle yields some of the most direct constraints available on the geometry of mantle flow. This is due to the causative link between deformation and anisotropy; when an aggregate of upper-mantle minerals is subjected to deformation (under certain conditions), it develops a crystallographic preferred orientation that, in turn, results in macroscopic seismic anisotropy (e.g. Karato *et al.* 2008). One of the least ambiguous indicators of anisotropy in the Earth's upper mantle is the birefringence or splitting of shear waves, which has emerged as a popular tool for characterizing anisotropy and mantle flow (for a recent review, see Long & Silver 2009). Although shear wave splitting is traditionally thought of as a single-station measurement, the increasing popularity of long-running, high-quality arrays of broad-band seismometers means that splitting measurements can often be treated in the context

of dense array data (e.g. Long & Silver 2009) and can be interpreted in increasingly sophisticated ways. This includes the development and implementation of techniques for the tomographic inversion of shear wave splitting measurements for complex anisotropic structure at depth (e.g. Chevrot 2006; Abt & Fischer 2008; Long *et al.* 2008). There have also been attempts to compare and synthesize constraints on azimuthal anisotropy obtained from different types of observations, particularly shear wave splitting and surface wave inversions (e.g. Simons *et al.* 2002; Li *et al.* 2003). Very recently, joint inversions of splitting and surface wave observations for anisotropic structure have been implemented (Marone & Romanowicz 2007; Yuan & Romanowicz 2010), and there has also been work that considers how to invert jointly different types of data for azimuthal anisotropy from a finite-frequency point of view (Panning & Nolet 2008).

A complete treatment of shear wave splitting data sets—and a full description of the geometry of anisotropy at depth—requires a correct description of the behaviour of shear waves in a vertically stratified anisotropic medium. In the presence of multiple

*Deceased.

layers of anisotropy, a (nearly) vertically propagating shear wave will be affected by successive layers of anisotropy, and the measured splitting parameters (fast direction, ϕ , and delay time, δt) cannot be simply related to the geometry of any one layer, as they can in the simplest case of a single, laterally homogeneous layer of anisotropy with a horizontal axis of symmetry. Several different studies have sought to understand shear wave splitting behaviour in a vertically stratified medium (e.g. Silver & Savage 1994; Brechner *et al.* 1998; Rumpker & Silver 1998; Wolfe & Silver 1998; Montagner *et al.* 2000; Saltzer *et al.* 2000). In particular, Silver & Savage (1994) and Montagner *et al.* (2000) each propose a theoretical treatment for predicting shear wave splitting parameters in the presence of multiple anisotropic layers, and each of these theoretical frameworks finds common use in the anisotropy literature (e.g. Liu *et al.* 1995; Levin *et al.* 1999; Walker *et al.* 2001; Simons *et al.* 2002; Li *et al.* 2003; Marone and Romanowicz 2007; Wüstefeld *et al.* 2009). There is a fundamental discrepancy, however, between Silver & Savage (1994) and Montagner *et al.* (2000) on the question of whether the splitting operator can be treated as commutative in the low-frequency limit. In particular, the treatment of Silver & Savage (1994) implies that the splitting operator does not commute even at low frequency, while Montagner *et al.* (2000) assert that the higher order terms that lead to this non-commutativity can be discarded in the low-frequency limit.

In this paper we investigate the source of this discrepancy and show that the splitting operator must be treated as non-commutative at frequencies relevant to the case of teleseismic shear wave splitting due to (weak) upper-mantle anisotropy. (For typical shear wave splitting studies, characteristic periods of the waves under study are ~ 8 – 12 s, while resolvable upper-mantle shear wave splitting delay times are typically ~ 0.5 – 2 s.) We illustrate this non-commutativity with a simple forward modelling exercise, computing synthetic seismograms via a particle motion perturbation method for a two-layer anisotropy model and comparing them to the predictions made by expressions derived by Silver & Savage (1994) and elaborated upon here. Finally, we discuss the implications of the non-commutativity of the shear wave splitting operator for the tomographic inversion of splitting measurements (and other types of seismic observations such as surface wave dispersion) for heterogeneous models of anisotropic structure at depth.

2 SHEAR WAVE SPLITTING IN STRATIFIED ANISOTROPIC MEDIA: THEORY

To make the comparison between the theoretical treatments of Silver & Savage (1994) and Montagner *et al.* (2000), it is most convenient to use the notation of Silver & Savage (1994) and to consider initially the case of two anisotropic layers and then generalize to the multilayer case. We first consider the case of a (nearly) vertically propagating shear phase with an initial linear polarization; for the commonly used SKS phases, the initial polarization is in the direction of the backazimuth, while for direct S phases it is controlled by the source mechanism. We seek to describe the splitting of an incident shear wave $\mathbf{u}(\omega)$ with initial polarization direction $\hat{\mathbf{p}}$ using the concept of the splitting operator Γ (e.g. Silver & Chan 1991). The splitting operator describes the effect of splitting of the incident shear wave due to an anisotropic layer onto the fast and slow polarization directions ($\hat{\mathbf{f}}$ and $\hat{\mathbf{s}}$, respectively) with a time shift of δt . This splitting operator can be written as

$$\Gamma = e^{i\omega\delta t/2}\hat{\mathbf{f}}\hat{\mathbf{f}} + e^{-i\omega\delta t/2}\hat{\mathbf{s}}\hat{\mathbf{s}}, \quad (1)$$

and the split shear wave $\mathbf{u}_s(\omega)$ can be written as

$$\mathbf{u}_s(\omega) = w(\omega)\Gamma \cdot \hat{\mathbf{p}}, \quad (2)$$

where $w(\omega)$ is the wavelet function. We seek to describe the apparent splitting parameters ϕ_a and δt_a due to the effect of multiple layers of anisotropy; we let $\alpha_{1,2} = 2\phi_{1,2}$, where $\phi_{1,2}$ is the angle between the initial polarization direction $\hat{\mathbf{p}}$ and the fast direction of each layer, and $\theta_{1,2} = \omega\delta t_{1,2}/2$, where δt is the delay time associated with each layer. For two layers, the expression that describes splitting in terms of the fast polarization direction and delay time of the individual layers may be written (Silver & Savage 1994, eq. A6).

$$\Gamma_1 \cdot \Gamma_2 \cdot \hat{\mathbf{p}} = (a_p + iC_c)\hat{\mathbf{p}} + (a_{p\perp} + iC_s)\hat{\mathbf{p}}_{\perp}, \quad (3)$$

where

$$a_p = \cos\theta_1 \cos\theta_2 - \sin\theta_1 \sin\theta_2 \cos(\alpha_2 - \alpha_1) \quad (4)$$

$$a_{p\perp} = -\sin\theta_1 \sin\theta_2 \sin(\alpha_2 - \alpha_1) \quad (5)$$

$$C_c = \cos\theta_1 \sin\theta_2 \cos\alpha_2 + \cos\theta_2 \sin\theta_1 \cos\alpha_1 \quad (6)$$

$$C_s = \cos\theta_1 \sin\theta_2 \cos\alpha_2 + \cos\theta_2 \sin\theta_1 \sin\alpha_1, \quad (7)$$

and $\hat{\mathbf{p}}$, $\hat{\mathbf{p}}_{\perp}$ are the radial and transverse directions, respectively. Montagner *et al.* (2000) established expressions for the apparent splitting parameters (α_a , θ_a) at long periods (that is, when the delay time δt is much smaller than the characteristic period of the wave under study). This was done by evaluating an expression similar to (3) and retaining terms to first order in ω . At long periods ($\theta_i \ll 1$),

$$a_p \approx 1, \quad (8)$$

$$a_{p\perp} \approx -\theta_1\theta_2 \sin(\alpha_2 - \alpha_1), \quad (9)$$

$$C_c \approx \theta_2 \cos\alpha_2 + \theta_1 \cos\alpha_1, \quad (10)$$

$$C_s \approx \theta_2 \sin\alpha_2 + \theta_1 \sin\alpha_1, \quad (11)$$

and thus, to first order, eq. (3) can be rewritten as

$$\Gamma_1 \cdot \Gamma_2 \cdot \hat{\mathbf{p}} \approx (1 + iC_c)\hat{\mathbf{p}} + iC_s\hat{\mathbf{p}}_{\perp}. \quad (12)$$

This expression is equivalent to eq. (19) of Montagner *et al.* (2000) and they used this to calculate the apparent splitting parameters

$$\tan\alpha_a = C_s/C_c, \quad (13)$$

$$\tan\theta_a = \sqrt{C_c^2 + C_s^2}, \quad (14)$$

which correspond to eqs (22) and (21) of Montagner *et al.* (2000), respectively. (Recall that $\alpha_a = 2\phi_a$ and $\theta_a = \omega\delta t_a/2$.) In this formulation, the splitting operators for each layer appear to commute, since neither C_s nor C_c changes upon reversal of the order of the splitting operators.

The other approach, taken by Silver & Savage (1994) and others (e.g. Rumpker & Silver 1998; Wolfe & Silver 1998), is to retain all terms in the displacement expression (3), derive an expression for the apparent splitting parameters and then evaluate these expressions for the low-frequency case. We demonstrate here that these two approaches lead to fundamentally different results. For the two-layer case, the full expressions for the apparent splitting parameters are (Silver & Savage 1994, eqs 7 and 8)

$$\tan\alpha_a = \frac{a_{p\perp}^2 + C_s^2}{a_p a_{p\perp} + C_s C_c}, \quad (15)$$

$$\tan \theta_a = \frac{\sqrt{(a_p a_{p\perp} + C_s C_c)^2 + (a_{p\perp}^2 + C_s^2)^2}}{a_p C_s - a_{p\perp} C_c}. \quad (16)$$

Taking these expressions in the same low-frequency approximation, we obtain

$$\tan \alpha_a = \frac{C_s^2}{a_{p\perp} + C_s C_c}, \quad (17)$$

$$\tan \theta_a = \sqrt{(a_{p\perp}/C_s + C_c)^2 + C_s^2}. \quad (18)$$

Note that if the term $a_{p\perp}$ is set to zero, then eqs (17) and (18) reduce to (13) and (14), respectively. The case where $a_{p\perp} = 0$ corresponds to the case where the delay time is zero, the period of the wave under study is infinitely large, or the angle between the layers is zero. In this case, the formulations of Silver and Savage (1994) and Montagner *et al.* (2000) are equivalent.

We can generalize the expressions (4)–(7) for the case of multiple layers (after Silver & Savage 1994).

$$a_p = S \left[1 - \sum_{n=1}^{N-1} \sum_{n'=n+1}^N \tan \theta_n \tan \theta_{n'} \cos(\alpha_n - \alpha_{n'}) + O(\tan^4 \theta) \right], \quad (19)$$

$$a_{p\perp} = S \left[\sum_{n=1}^{N-1} \sum_{n'=n+1}^N \tan \theta_n \tan \theta_{n'} \sin(\alpha_n - \alpha_{n'}) + O(\tan^4 \theta) \right], \quad (20)$$

$$C_c = S \left[\sum_{n=1}^N \tan \theta_n \cos \alpha_n + O(\tan^3 \theta) \right], \quad (21)$$

$$C_s = S \left[\sum_{n=1}^N \tan \theta_n \sin \alpha_n + O(\tan^3 \theta) \right], \quad (22)$$

where

$$S = \prod_{n=1}^N \cos \theta_n; \quad (23)$$

here N is the number of layers. (We note that only the terms proportional to $\tan \theta$ or $\tan^2 \theta$ must be retained.) In the case where the delay time is much smaller than the characteristic period ($\theta_i \ll 1$) these expressions simplify to

$$a_p \approx 1, \quad (24)$$

$$a_{p\perp} \approx \sum_{n=1}^{N-1} \sum_{n'=n+1}^N \theta_n \theta_{n'} \sin(\alpha_n - \alpha_{n'}), \quad (25)$$

$$C_c \approx \sum_{n=1}^{N-1} \theta_n \cos \alpha_n, \quad (26)$$

$$C_s \approx \sum_{n=1}^{N-1} \theta_n \sin \alpha_n. \quad (27)$$

The difference in the formulations of Silver & Savage (1994) and Montagner *et al.* (2000) thus comes down to whether or not the term $a_{p\perp}$ must be retained at frequencies relevant to studies of upper-mantle anisotropy using shear wave splitting. It is this term, and this term only, that controls the commutivity of the splitting

operators (as well as the frequency dependence). In the expression that describes the application of the splitting operators (eq. 3), $a_{p\perp}$ is second order in ω , which is why it was discarded in the analysis of Montagner *et al.* (2000). Yet, it is clear from eqs (17) and (18) that the term including $a_{p\perp}$ is of the same order as the other terms that have been retained, and thus cannot be discarded. Therefore, a complete treatment of splitting due to multiple anisotropic layers requires that the splitting operators be treated as non-commutative. (Recall that for the end-member case of vanishingly small delay times or infinitely large periods, the term $a_{p\perp}$ goes to zero. A discussion of shear wave splitting measurement methods, their detection limits and the frequencies at which the non-commutivity of splitting operators is relevant can be found in Section 3.)

The implications of this non-commutivity for the interpretation of shear wave splitting measurements in the presence of vertically stratified anisotropy are substantial. First, as pointed out by Silver & Savage (1994), the fact that the splitting operators associated with multiple anisotropic layers do not commute implies that the back-azimuthal variation in apparent splitting parameters can be used not only to diagnose multiple layers of anisotropy, but to determine their order. This property is commonly exploited in shear wave splitting studies that infer the presence of two or more layers (e.g. Savage & Silver 1993; Özalaybey & Savage 1994; Liu *et al.* 1995; Levin *et al.* 1999; Walker *et al.* 2001; Snyder & Bruneton 2007), but it is inconsistent with the theoretical framework proposed by Montagner *et al.* (2000), which does not predict any backazimuthal variation in apparent splitting parameters in the presence of multiple layers of anisotropy. A second implication of the non-commutivity demonstrated by eqs (17) and (18) is that the expressions derived by Montagner *et al.* (2000) for predicting *SKS* splitting parameters from anisotropic models derived from surface wave observations yield incomplete results for the case where the fast direction changes substantially with depth. Silver & Savage (1994) demonstrated that the backazimuthal variations in apparent splitting parameters induced by the non-commutivity of the splitting operator are most dramatic when the delay times associated with each layer are not dramatically different and the offset in fast directions between layers is between $\sim 30^\circ$ – 60° ; in other cases, the effects are more subtle and the expressions of Montagner *et al.* (2000) provide a fairly accurate approximation of the effects of multiple layers. The non-commutivity of the splitting operator may explain, in part, why attempts to reconcile anisotropic models obtained from surface waves with *SKS* splitting measurements using the Montagner *et al.* (2000) expressions (e.g. Simons *et al.* 2002; Li *et al.* 2003) have not been entirely successful. A third implication is that shear wave splitting measurements and surface wave observations cannot be correctly integrated in a joint inversion for anisotropic structure using the Montagner *et al.* (2000) approximations if there is a substantial change in the fast axis direction with depth, unless the measurements are made at very long periods. The accuracy of tomographic models obtained via such a joint inversion (e.g. Marone & Romanowicz 2007; Yuan & Romanowicz 2010) may be degraded in regions of the model where the fast directions change substantially with depth; however, if the fast directions vary with depth by less than $\sim 30^\circ$, then the violations of the assumptions made would be less severe, and such regions of the anisotropic model would generally be reliable.

Although the shear wave splitting operator Γ does not commute, it is possible to identify a combination of apparent splitting parameters (known as the splitting intensity) that does indeed commute in the low-frequency limit, as pointed out by Chevrot (2000) and elaborated upon by several workers (e.g. Chevrot 2006; Long *et al.*

2008; Sieminski *et al.* 2008). We write expressions for combinations of the apparent splitting parameters θ_a and α_a that are valid at any frequency.

$$\tan \theta_a \sin \alpha_a = \frac{a_{p\perp}^2 + C_s^2}{a_p C_s - a_{p\perp}^2 C_c}, \quad (28)$$

$$\tan \theta_a \cos \alpha_a = \frac{a_p a_{p\perp} + C_s C_c}{a_p C_s - a_{p\perp}^2 C_c}. \quad (29)$$

In the low-frequency limit, $a_{p\perp} \ll a_p$ and $a_{p\perp} \ll C_s$, so eqs (28) and (29) reduce to these approximate expressions.

$$\tan \theta_a \sin \alpha_a \approx C_s, \quad (30)$$

$$\tan \theta_a \cos \alpha_a \approx C_c + a_{p\perp}/C_s. \quad (31)$$

The expression $\tan \theta_a \sin \alpha_a$, which corresponds to the splitting intensity defined by Chevrot (2000), does commute in the low-frequency limit and can be used as an observable for the tomographic inversion of shear wave splitting measurements (Chevrot 2006; Long *et al.* 2008; Sieminski *et al.* 2008; Chevrot & Monteiller 2009) and as the basis for the joint inversion of surface wave and shear wave splitting observations for anisotropic models (Panning & Nolet 2008). The closely related quantity $\tan \theta_a \cos \alpha_a$, which we denote as the complimentary splitting intensity, does not commute in the low-frequency limit.

3 MEASUREMENT METHODS AND FREQUENCY CONTENT: PRACTICAL CONSIDERATIONS

Eqs (17) and (18) describe the backazimuthal dependence of apparent splitting parameters in the presence of multiple anisotropic layers, but to assess the relevance of the non-commutivity of shear wave splitting operators for actual data sets it is important to consider the frequency content of the waves under study as well as the methods used to obtain measurements of apparent splitting parameters. Several studies have sought to compare the performance of various splitting measurement methods for both synthetic and real data (e.g. Long & van der Hilst 2005a; Wüstefeld & Bokelmann 2007; Vecsey *et al.* 2008; Monteiller & Chevrot 2010), and a detailed overview of measurement methods for long-period teleseismic data can be found in Long & Silver (2009). Commonly used methods for measuring apparent splitting parameters (ϕ , δt) from a single seismogram include the transverse component minimization method of Silver & Chan (1991) and the closely related eigenvalue method, the rotation-correlation method (also known as the cross-correlation method) and the cross-convolution method of Menke & Levin (2003). Each method takes a different approach towards identifying the pair of splitting parameters that best accounts for the effect of anisotropy on the *SKS* (or *S*) waveform. The Silver & Chan (1991) methods seek to linearize the corrected particle motion after the effect of splitting has been removed, either by minimizing the corrected transverse component energy (if the initial polarization of the wave is known) or by identifying the most nearly singular time-domain covariance matrix through an eigenvalue-based measure. The rotation-correlation method seeks to maximize the correlation between the corrected fast and slow components, accommodating the prediction that the split waves should have identical pulse shapes. The cross-convolution method, in contrast, uses the

match between observed and predicted waveforms for hypothetical earth models to characterize anisotropic structure at depth, and does not need to rely on measurements of apparent splitting parameters. In theory, our equations for the variation of apparent splitting parameters in eqs (17) and (18) should be applicable for any of the measurement methods (transverse component minimization, eigenvalue or rotation-correlation) that measure apparent splitting parameters. However, several studies have demonstrated that in practice different measurement methods can yield different results for noisy data and/or in the presence of complex anisotropic structure (e.g. Levin *et al.* 2004; Long & van der Hilst 2005a), particularly when delay times are small, and the simultaneous application of several different methods can help to identify unstable measurements (e.g. Long & Silver 2009).

It is important to note that the single-record measurement methods, in particular, suffer from significant limitations in detecting splitting associated with small delay times in the presence of noise. For most *SKS* splitting studies, the characteristic periods of the waves under study is typically ~ 8 – 10 s, although for some arrivals there is significant energy at shorter or longer periods. For a characteristic period of ~ 10 s with noise levels that are typical for *SKS* splitting studies, single-record measurement methods will have a lower delay time detection limit of perhaps ~ 0.5 s (Long & Silver 2009, and references therein). For particularly high levels of noise, detection of weak splitting may be even more difficult; for example, Monteiller & Chevrot (2010) demonstrated that at a period of 12 s and low signal-to-noise ratios of 3–6, splitting with a delay time of 0.65 s could not be reliably detected using the transverse component minimization method. In contrast, estimates of splitting parameters derived from measurements of the splitting intensity (Chevrot 2000) can reliably characterize relatively smaller delay times (Monteiller & Chevrot 2010; see also Long & van der Hilst 2005a). In any case, it is important to keep in mind that the effect of very small splitting, with delay times extremely small compared to the characteristic period of the phase under study, on the waveforms of *SKS* arrivals (or other shear phases) is subtle, and very weak splitting is difficult to reliably characterize in the presence of realistic levels of noise.

The lower detection limit of frequently used shear wave splitting measurement methods is salient for understanding the practical importance of the non-commutivity of shear wave splitting operators. As discussed earlier, this non-commutivity is controlled by the term $a_{p\perp}$ appearing in eqs (17) and (18), which does not appear in the Montagner *et al.* (2000) formulation (eqs 13 and 14). In the end-member case of zero delay time or infinitely large periods, or in the case where the angle between the anisotropic layers is zero, the term $a_{p\perp}$ goes to zero and the two formulations are equivalent. The non-commutivity of shear wave splitting operators is therefore more important at larger delay times (relative to characteristic period) and for the case where the angle between the anisotropic layers at depth is large ($\sim 30^\circ$ – 60°). For the typical case of *SKS* (or teleseismic *S*) splitting due to upper-mantle anisotropy, where characteristic periods are ~ 8 – 10 s and delay times range up to ~ 2 – 2.5 s, non-commutivity in the presence of multiple anisotropic layers must be taken into account. For smaller delay times, the non-commutivity becomes less important, but at delay times less than perhaps ~ 0.5 s (depending on signal-to-noise ratio) the apparent splitting measurements cannot be reliably estimated in any case. At smaller delay times, the multichannel method is better able to estimate splitting parameters (Monteiller & Chevrot 2010), but in this case the splitting intensity measurement does in fact commute.

4 SYNTHETIC EXAMPLES USING FORWARD MODELLING

To illustrate the non-commutivity of the splitting operator Γ at relevant frequencies, we carry out a simple forward modelling exercise using noise-free synthetics generated using codes modified from those contained in the SynthSplit software package (http://www.geo.brown.edu/People/Grads/abt/Tools/SynthSplit_download.htm). The method used for efficiently approximating particle motion for multiply split shear waves, documented in Abt & Fischer (2008), is based on the particle motion perturbation method of Fischer *et al.* (2000) and has been benchmarked against full waveform synthetics computed using a pseudo-spectral technique (Abt & Fischer 2008). We tested two scenarios, each consisting of two simple two-layer anisotropic models, as shown in Fig. 1. In the first scenario, Model A consists of an anisotropic layer with fast direction N135°E associated with a delay time of 1.0 s that overlies a deeper layer with a fast direction of N90°E and a delay time of 1.4 s. This model is similar to that proposed to explain shear wave splitting patterns observed at station BKS in Berkeley, CA by Özalaybey & Savage (1995; see also Savage 1999). In Model B, the order of the layers is reversed. (The difference in associated delay time is implemented by keeping the elastic constants associated with orthorhombic anisotropy with a horizontal axis of symmetry the same and adjusting the thickness of the layer.) In the second scenario, the fast directions and relative delay times of the layers are the same as in Scenario 1, but the

absolute delay times are different. Model C is similar to Model A, but has a delay time of 0.5 s for the upper layer ($\phi = \text{N}135^\circ\text{E}$) and 0.7 s for the lower layer ($\phi = \text{N}90^\circ\text{E}$). In Model D, the order of the layers is reversed. Because the synthetic seismograms are computed for the same period (8 s) for both scenarios, the different absolute delay times in Scenario 1 versus Scenario 2 allows us to investigate the accuracy of the Silver & Savage (1994) expressions for different ratios of delay times to characteristic period.

We carry out synthetic seismogram modelling for a series of vertically propagating shear waves with a period of 8 s for a variety of initial polarization directions for each model. We measure the apparent shear wave splitting parameters ($\phi, \delta t$) using the eigenvalue minimization technique of Silver & Chan (1991) and compare the measurements from the synthetic seismograms with predictions of the backazimuthal variation in apparent splitting parameters for each model in the low-frequency limit evaluated using eqs (17) and (18). We simulate shear wave splitting for each of the anisotropic models for a vertically incident shear wave (zero slowness) with initial polarization parallel to the backazimuth. We model backazimuths from 0° to 180° in 10° increments; the initial waveform is a sinusoidal pulse with a period of 8 s (similar to a typical characteristic period for *SKS* phases). Each anisotropic layer is described using the elastic constants typical for single-crystal olivine, rotated to reflect the direction of the fast axis in the horizontal plane; the thickness of the layer is adjusted to produce the desired delay time.

Fig. 2 shows the splitting parameters ($\phi, \delta t$) measured from each of the synthetic seismograms as a function of backazimuth for each

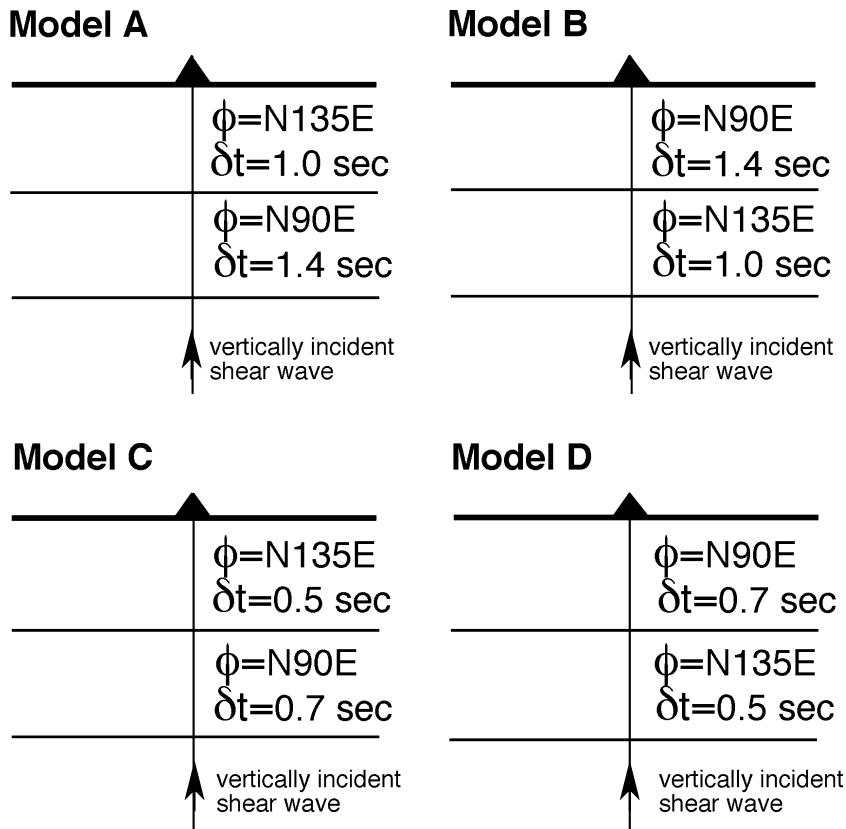


Figure 1. Sketch of two-layer models used in the synthetic seismogram calculations. In Scenario 1, Model A consists of an upper anisotropic layer with a fast direction of N135°E and a delay time of 1.0 s and a lower layer with a fast direction of N90°E and a delay time of 1.4 s. In Model B, the order of the layers is reversed. In Scenario 2, the fast directions and relative delay times of the layers are the same as in Scenario 1, but the absolute delay times are smaller. For Scenario 2, Model C has a delay time of 0.5 s for the upper layer ($\phi = \text{N}135^\circ\text{E}$) and 0.7 s for the lower layer ($\phi = \text{N}90^\circ\text{E}$). In Model D, the order of the layers is reversed.

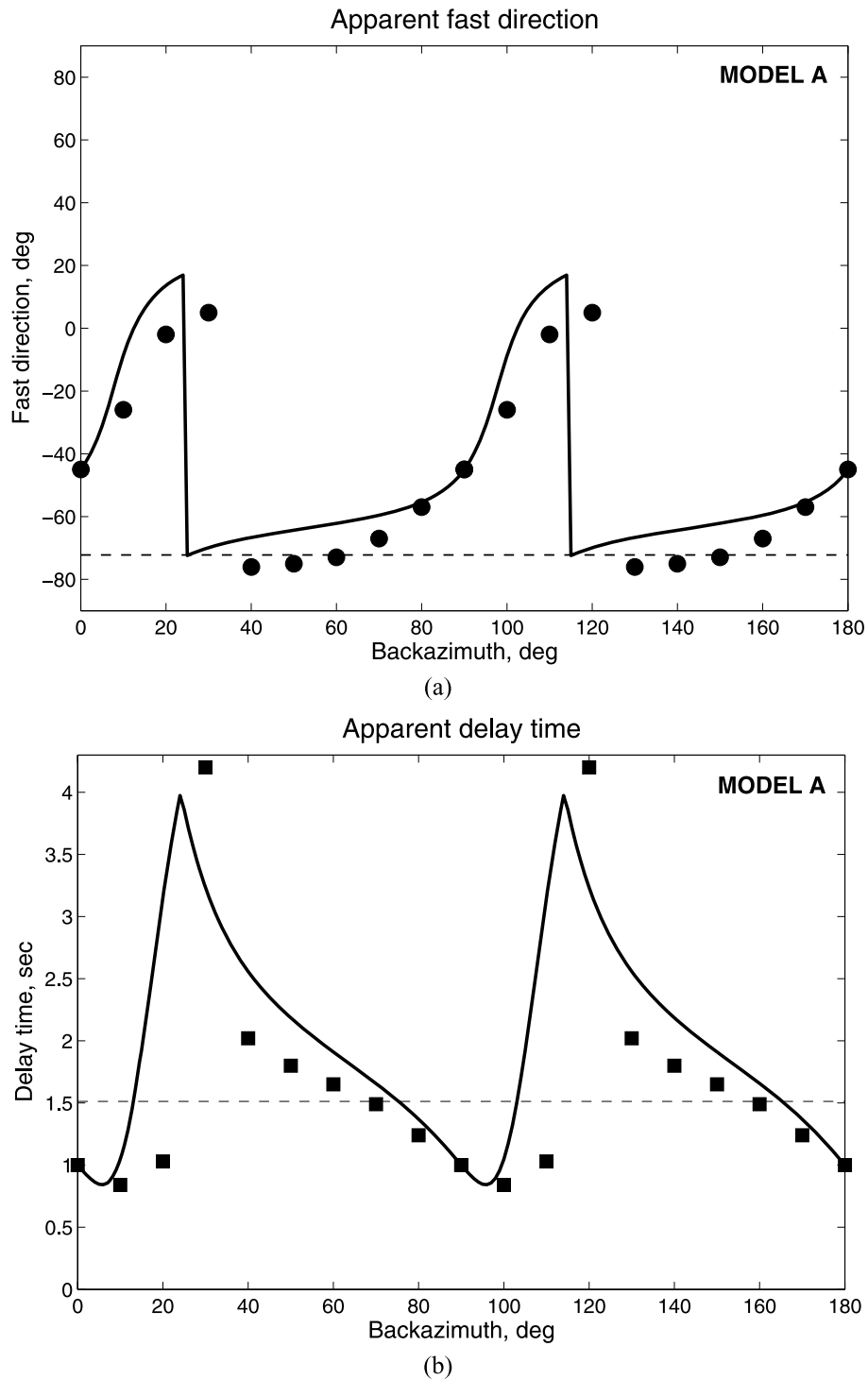


Figure 2. Predictions of the backazimuthal variation of apparent splitting parameters using the analytical equations of Silver & Savage (1994) for Models A and B (Scenario 1) shown in Fig. 1, along with synthetic splitting observations computed for a characteristic period of 8 s. The predicted variation of the apparent fast direction (a) and delay time (b) for Model A are shown as (solid line) as a function of backazimuth along with synthetic splitting measurements (circles for fast directions, squares for delay times). The dashed lines indicate the predictions of the Montagner *et al.* (2000) expressions, which are independent of the order of the layers. The same predictions for Model B are shown in (c) and (d).

model in Scenario 1 along with the variations predicted by eqs (17) and (18). The results for Model A are similar to those obtained by Savage (1999), who carried out reflectivity synthetic seismogram modelling for the same two-layer model used here. The apparent

splitting parameters predicted by Montagner *et al.* (2000) expressions, which do not vary with backazimuth and are the same for Model A and Model B, are also shown. Fig. 3 shows the splitting intensity measured from each of the synthetic seismograms

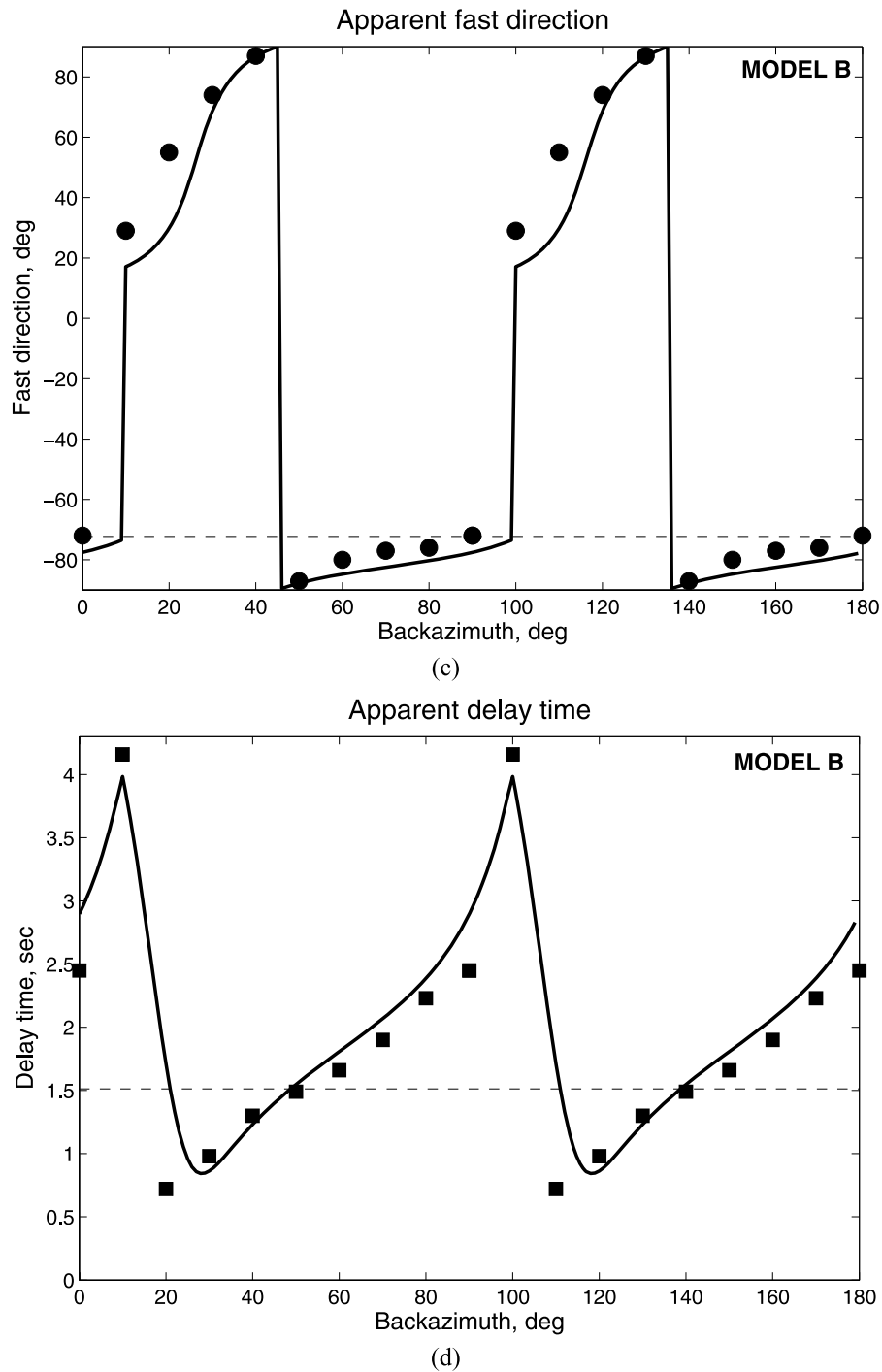


Figure 2. (Continued.)

for Scenario 1, along with the prediction obtained from summing the effects of each layer (e.g. Chevrot 2000). Because the splitting intensity is commutative, the predictions for Model A and Model B are the same. Figs 4 and 5 show the predictions and synthetic seismogram measurements for Scenario 2, with the same plotting conventions as Figs 2 and 3. This simple forward modelling exercise demonstrates that switching the order of the layers has a profound effect on the measured apparent splitting parameters and that the non-commutivity of the shear wave splitting operators must indeed be taken into account at frequencies typical of commonly used SKS phases.

5 IMPLICATIONS FOR ANISOTROPY TOMOGRAPHY

There are several implications of the non-commutivity of the splitting operator for the tomographic inversion of shear wave splitting measurements for anisotropic structure, which is receiving more attention as the availability of data from dense broad-band arrays increases (e.g. Ryberg *et al.* 2005; Chevrot 2006; Abt & Fischer 2008; Long *et al.* 2008; Abt *et al.* 2009). The first important implication is that the combination of surface wave and shear wave splitting observations in tomographic inversions for anisotropic structure

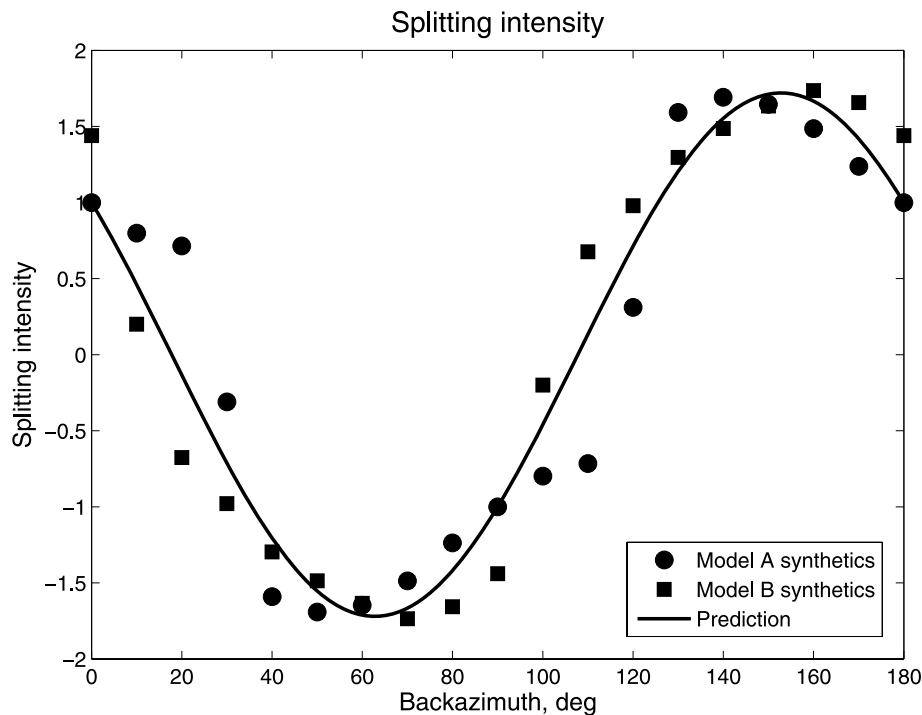


Figure 3. Predictions of the splitting intensity (solid line) for the two-layer models (A and B) in Scenario 1 (Fig. 1) obtained by summing the predictions for each layer (Chevrot 2000) along with measurements of the splitting intensity as a function of backazimuth from the synthetic seismograms computed in the forward modelling exercise for Model A (circles) and Model B (squares). Because the splitting intensity is commutative, the predictions for Model A and Model B are the same.

must be carried out with extreme care. In particular, the expressions derived by Montagner *et al.* (2000) to relate body wave and surface wave anisotropy are useful approximations in the case where the measured splitting parameters do not vary significantly with backazimuth, which would imply that the fast directions in the model are relatively homogeneous with depth, but they can be misleading in cases where these conditions are violated. Because these expressions do not take into account the non-commutivity of the splitting operator, they do not correctly relate very complex anisotropic structure at depth to observations of apparent splitting parameters at the surface. Anisotropic tomographic models that have been obtained by jointly inverting surface wave and *SKS* splitting observations using the Montagner *et al.* (2000) expressions (e.g. Marone & Romanowicz 2007) should be treated with some caution in regions of the model where the fast anisotropic direction varies significantly with depth.

In contrast to the splitting operator Γ , the so-called splitting intensity $\tan \theta_a \sin \alpha_a$ is commutative and can be treated as such in a tomographic inversion framework. The utility of measuring the amount of energy on the transverse component of *SKS* waves relative to the radial component was first pointed out by Vinnik *et al.* (1989) and was incorporated into the so-called multichannel measurement method by Chevrot (2000), who advocated measuring the splitting intensity at a variety of backazimuths and fitting a $\sin 2\beta$ curve to the measurements to identify the best-fitting splitting parameters (ϕ , δt). This measurement method has been applied to several real-world data sets (e.g. Long & van der Hilst 2005b; Lev *et al.* 2006; Kummerow & Kind 2006), but perhaps the most powerful application of the splitting intensity measurement lies in its suitability for tomographic imaging of anisotropic structure (Chevrot 2006; Long *et al.* 2008; Sieminski *et al.* 2008; Chevrot & Monteiller 2009). Because the splitting intensity measurement is commutative,

it can be treated analogously to a body wave traveltime in isotropic wave speed tomography; in particular, finite-frequency sensitivity kernels for splitting intensity observations can be computed in a manner very similar to those for traveltimes measured by waveform cross-correlation (Favier & Chevrot 2003; Favier *et al.* 2004; Chevrot 2006; Long *et al.* 2008). If shear wave splitting intensity measurements can be collected for a dense network of stations for a variety of *SKS* and/or direct teleseismic *S* ray paths, which include different incoming polarization angles and incidence angles, then images of upper-mantle anisotropy can be obtained in a manner very similar to traditional traveltime tomography. Indeed, even if only *SKS* measurements with nearly vertical ray paths are used, sufficient resolution of upper-mantle structures can be obtained if finite-frequency theory is applied and the station spacing is sufficiently dense (Chevrot & Monteiller 2009), as the sensitivity kernels for different observations will overlap at depth.

Splitting intensity measurements are extremely well suited for the problem of imaging anisotropy, but they do suffer from the key disadvantage of ‘losing’ homogeneous anisotropic layers at depth (e.g. Chevrot & Monteiller 2009). Consider the two-layer models shown in Fig. 1—traditional measurements of apparent splitting parameters (ϕ_a , δt_a) will exhibit a backazimuthal variation that is characteristic of two anisotropic layers with a significant (45°) offset in fast direction, and the character of that variation can be used to infer the order of the layers (Figs 2 and 4). In contrast, measurements of the splitting intensity for such a model are not distinguishable from a model with a single layer of anisotropy, and the splitting intensity observations will not be affected if the order of the layers is switched (Figs 3 and 5). (This situation is analogous to the information contained in body wave traveltimes that are used to construct isotropic tomographic models. For the isotropic case, a laterally homogeneous layer of anomalous wave

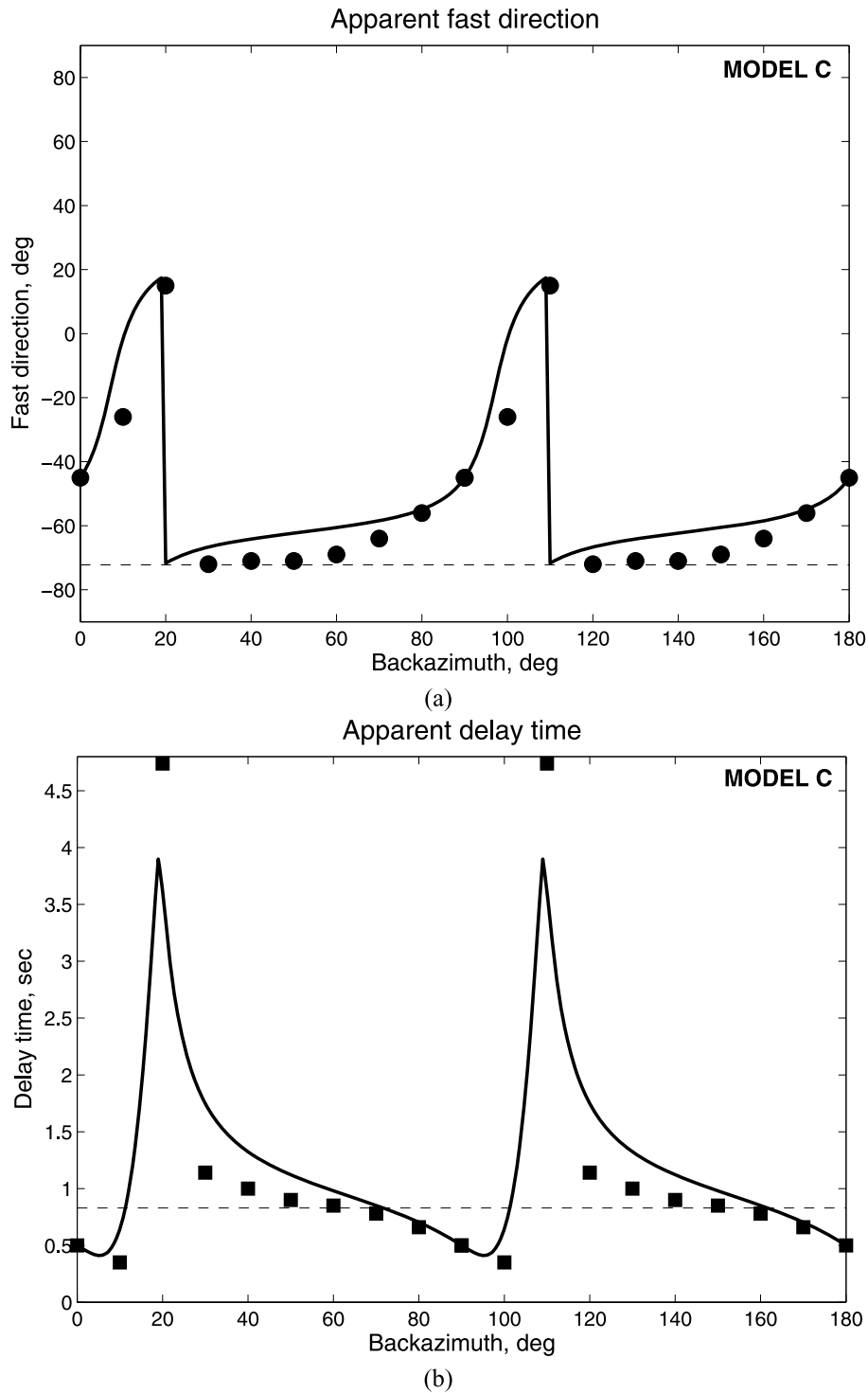


Figure 4. Predictions of the backazimuthal variation of apparent splitting parameters using the analytical equations of Silver & Savage (1994) for Models C and D (Scenario 2) shown in Fig. 1, along with synthetic splitting observations computed for a characteristic period of 8 s. Symbols are as in Fig. 2.

speed at depth would not result in travelt ime residuals along a seismic array, and a tomographic inversion would be insensitive to such a layer.) In practice, this implies that there is information contained in the apparent shear wave splitting parameters ($\phi_a, \delta t_a$) that is lost in the splitting intensity measurement. Put another way, the fact that the splitting operator Γ is non-commutative implies that in the presence of complex anisotropy, the apparent shear wave

splitting parameters do, in fact, contain some information about the depth distribution of anisotropic structure.

A key question, therefore, is whether there is a way to use the ‘additional’ information contained in the apparent splitting parameters in tomographic inversions for anisotropic structure. One approach is to construct the tomographic inversion in a way that explicitly takes into account the non-commutivity of the splitting operator. For

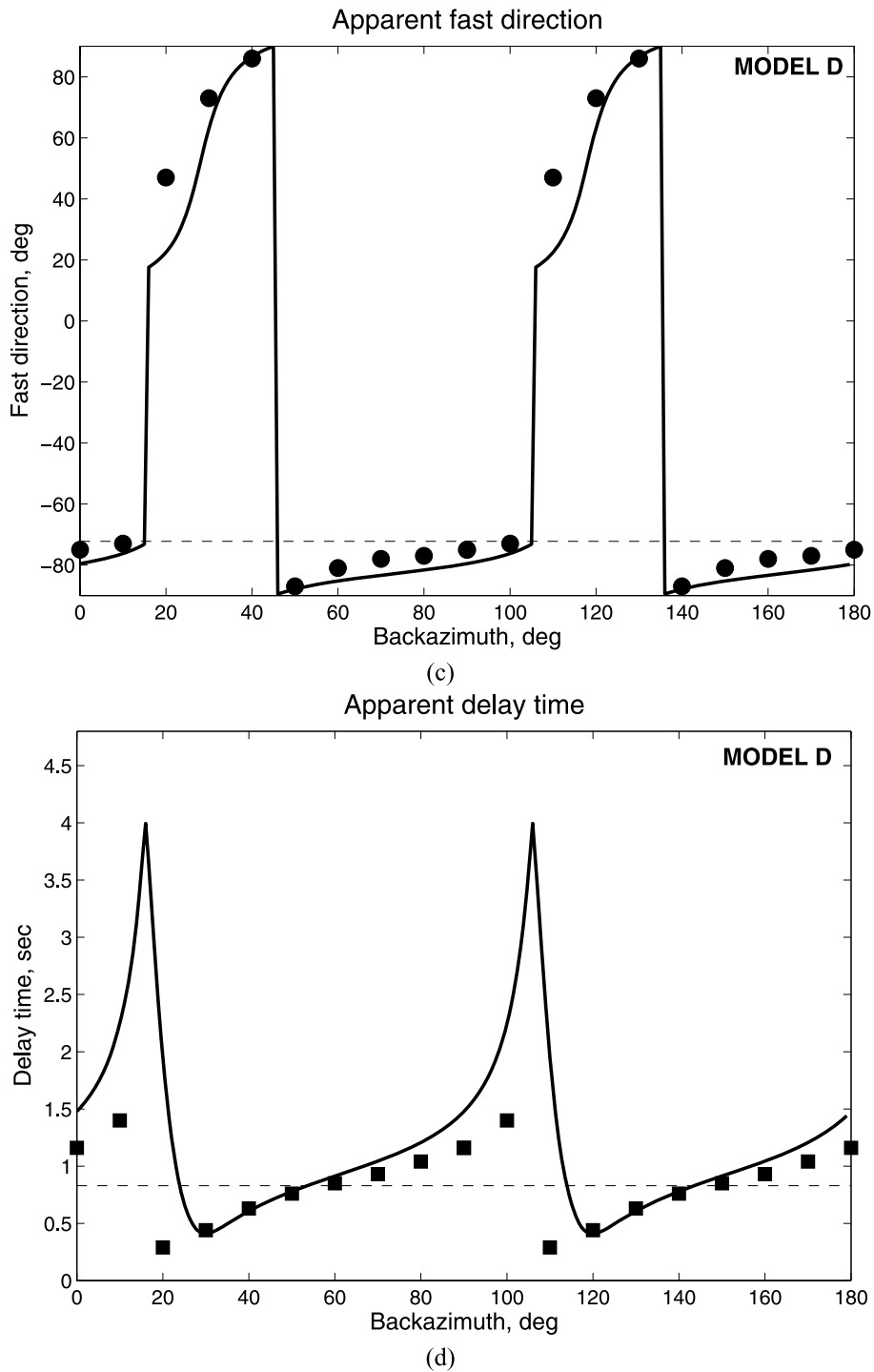


Figure 4. (Continued.)

example, Abt & Fischer (2008) proposed a ray-theoretical method for shear wave splitting tomography in which the partial derivatives that relate changes in anisotropic structure at depth to changes in apparent splitting parameters observed at the surface are calculated such that the propagation history of each ray is taken into account; the partial derivatives depend on the geometry of anisotropy both in the ‘block’ of the model in question and on the other blocks that have been previously sampled by the ray. The drawback of this approach is that the partial derivatives – and therefore the inver-

sion result – are highly dependent on the starting model. However, since tomographic inversions for anisotropic structure are by their very nature highly non-linear, the (linearized) sensitivities will depend heavily on the starting model even if the splitting intensity is used as the observable (Long *et al.* 2008). For inversions that rely upon splitting intensity measurements, the additional information contained in the apparent splitting parameters ($\phi_a, \delta t_a$) may still be used; one approach would be to validate the tomographic models obtained by splitting intensity tomography by predicting ($\phi_a, \delta t_a$) and

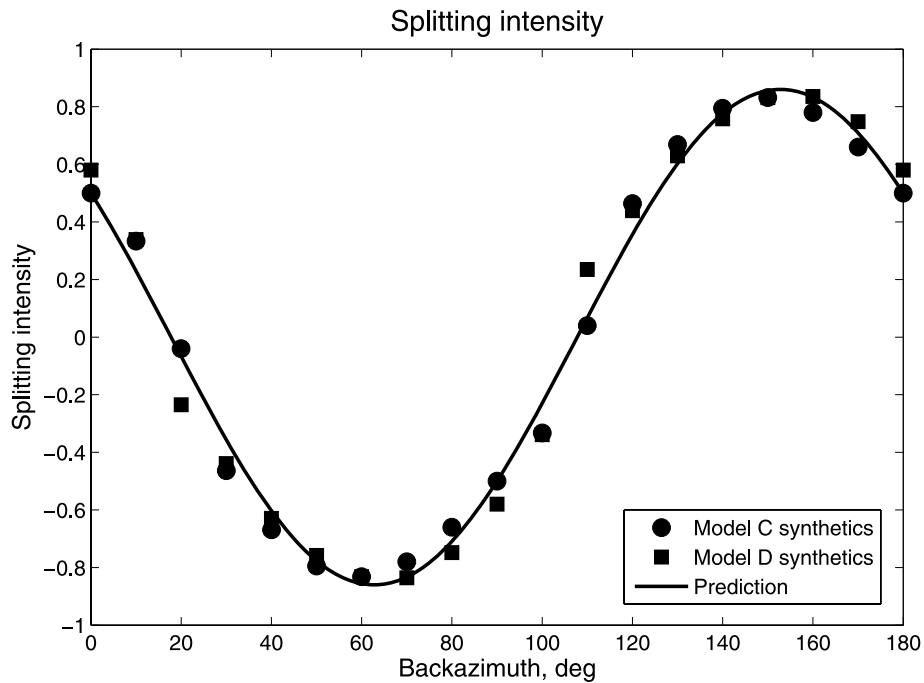


Figure 5. Predictions of the splitting intensity for the two-layer models (C and D) in Scenario 2 (Fig. 1). Symbols are as in Fig. 3.

comparing them to observations. This may help to identify aspects of the data that are not well-described by the tomographic model and may help to identify features (such as a “hidden” homogeneous layer of anisotropy at depth) that do not affect the splitting intensity measurements. Another approach would be to compare observations of the splitting intensity and apparent splitting parameters before implementing an inversion framework; if the apparent splitting data suggest a level of complexity that is not immediately apparent from the visual examination of the splitting intensity patterns, this may indicate the need for multiple layers of anisotropy to explain the data. Multiple layers of anisotropy at depth can also be diagnosed and characterized by detailed examination of the *SKS* waveforms, as in the cross-convolution method (Menke & Levin 2003). This information could be explicitly incorporated in a splitting intensity tomography inversion through the construction of a realistic background model (based on apparent splitting measurements ϕ_a and δt_a for different backazimuths) which serves as a starting point for the calculation of sensitivity kernels and the inversion of splitting intensity data (e.g. Long *et al.* 2008).

Although there are several potential strategies for exploiting the non-commutivity of shear wave splitting operators to characterize complex anisotropic structure at depth, it is important to keep in mind that from a practical point of view, the applicability of these strategies may be limited by the quality of the measurements themselves. Several studies have noted that single-record measurements such as the Silver & Chan (1991) methods or the rotation-correlation method tend to be less stable on real, noisy data than splitting intensity measurements (e.g. Chevrot 2000; Long & van der Hilst 2005a; Long & Silver 2009; Monteiller & Chevrot 2010), particularly in the presence of complex anisotropic structure (Long & van der Hilst 2005a). In practice, this means that robust, well-constrained measurements may be difficult to obtain, particularly for incoming polarization azimuths where the amount of energy on the uncorrected transverse component is small. An additional restriction that is particularly acute for *SKS* splitting data is the often limited back-

azimuthal distribution of sources in the distance region appropriate for *SKS* analysis, which can hamper a complete characterization of backazimuthal variations such as those shown in Figs 2 and 4. It is vital, therefore, to carefully assess the quality of a given shear wave splitting data set (in terms of noise levels, waveform complexity, size of errors on individual measurements, and (dis)agreement among different measurement methods) before implementing strategies for tomographic inversion.

We note, finally, that the suitability of the splitting intensity measurement for anisotropy imaging also provides a promising avenue for the joint inversion of surface wave and shear wave splitting measurements. Because the splitting intensity is commutative, it can be more easily combined with different types of seismological observables in an inversion framework. For example, Panning & Nolet (2008) suggested a (strongly reduced) parametrization scheme for finite-frequency anisotropic surface wave tomography and noted that such a strategy could accommodate the joint inversion of surface waves and splitting intensity observations. (An earlier reduced parametrization scheme for imaging seismic anisotropy was suggested by Becker *et al.* 2006.) This combination of different types of observations is likely to be particularly powerful, since the sensitivities of body waves and surface waves to anisotropic parameters are different (e.g. Sieminski *et al.* 2007) and they should provide complementary constraints on anisotropic structure at depth. *A priori* constraints on vertically stratified anisotropy from surface waves can also serve as a useful starting point for tomographic inversions of splitting intensity; multiple-layer surface wave models can be used as starting models in splitting intensity tomography and this combination can help to alleviate the problem of ‘losing’ homogeneous layers of anisotropy described earlier. Because of the differences in the commutative properties of the splitting operator Γ and the splitting intensity measurement, we view observations of splitting intensity as the most promising avenue for the joint inversion of surface wave and body wave observations for anisotropy models.

6 CONCLUSIONS

In this paper we have investigated the source of the discrepancy between the theoretical treatments of Silver & Savage (1994) and Montagner *et al.* (2000), both of which make predictions of apparent shear wave splitting parameters for anisotropic models with multiple layers of anisotropy in the low-frequency limit. We find that the discrepancy over whether or not the shear wave splitting operator can be treated as commutative arises from a difference in when the low-frequency approximation is applied, and show that the term in the apparent splitting parameter expressions that controls the non-commutivity is of the same order as other terms and must be retained at frequencies relevant for typical shear wave splitting studies of upper-mantle anisotropy. The expressions proposed by Montagner *et al.* (2000) are a valid approximation for cases in which the fast axis does not vary dramatically with depth, in which case large variations in apparent splitting parameters with backazimuth are not expected. When these conditions are violated, however, the framework of Montagner *et al.* (2000) may give inaccurate estimates of apparent splitting. The finding that the splitting operator must be treated as non-commutative at low frequencies has profound implications for studies that seek to reconcile anisotropic models derived from surface wave observations with shear wave splitting data, and for studies that attempt a joint tomographic inversion of surface wave and splitting observations for anisotropic models. The non-commutivity of the splitting operator also implies that the tomographic inversion of shear wave splitting measurements must be implemented with care, and the non-commutivity must be explicitly taken into account when calculating the partial derivatives for use in a linearized tomography problem. In contrast to the splitting operator, the quantity known as the splitting intensity (usually measured by cross-correlating the radial and transverse components of the shear arrival) does commute and can be treated in a tomographic framework in a manner similar to body wave traveltimes in isotropic tomography. Splitting intensity observations may also be combined with surface wave measurements into joint anisotropic tomography inversions in a relatively straightforward manner.

ACKNOWLEDGMENTS

We thank Thorsten Becker for helpful discussions regarding the prediction of splitting from surface wave models with multiple anisotropic layers and Martha Savage for valuable comments on a draft of this manuscript. We thank David Abt for making his codes for computing shear wave splitting in multiple anisotropic layers freely available. Thoughtful comments by reviewers Sebastien Chevrot and Jim Gaherty helped to improve the paper. This work was supported by the Department of Terrestrial Magnetism, Carnegie Institution of Washington and by NSF grant EAR-0911286 (MDL).

REFERENCES

- Abt, D.L. & Fischer, K.M., 2008. Resolving three-dimensional anisotropic structure with shear-wave splitting tomography, *Geophys. J. Int.*, **173**, 859–886.
- Abt, D.L., Fischer, K.M., Abers, G.A., Strauch, W., Protti, J.M. & Gonzalez, V., 2009. Shear-wave anisotropy beneath Nicaragua and Costa Rica: implications for flow in the mantle wedge, *Geochem. Geophys. Geosyst.*, **10**, Q05S15, doi:10.1029/2009GC002375.
- Becker, T.W., Chevrot, S., Schulte-Pelkum, V. & Blackman, D.K., 2006. Statistical properties of seismic anisotropy predicted by upper mantle geodynamic models, *J. geophys. Res.*, **111**, B08309, doi:10.1029/2005JB004095.
- Brechner, S., Klinge, K., Krüger, F. & Plenefisch, T., 1998. Backazimuthal variations of splitting parameters of teleseismic SKS phases observed at the broadband stations in Germany, *Pure appl. Geophys.*, **151**, 305–331.
- Chevrot, S., 2000. Multichannel analysis of shear wave splitting, *J. geophys. Res.*, **105**, 21 579–21 590.
- Chevrot, S., 2006. Finite-frequency vectorial tomography: a new method for high-resolution imaging of upper mantle anisotropy, *Geophys. J. Int.*, **165**, 641–657.
- Chevrot, S. & Monteiller, V., 2009. Principles of vectorial tomography: the effects of model parameterization and regularization in tomographic imaging of seismic anisotropy, *Geophys. J. Int.*, **179**, 1726–1736.
- Favier, N. & Chevrot, S., 2003. Sensitivity kernels for shear wave splitting in transverse isotropic media, *Geophys. J. Int.*, **153**, 213–228.
- Fischer, K.M., Parmentier, E.M., Stein, A.R. & Wolf, E.R., 2000. Modeling anisotropy and plate-driven flow in the Tonga subduction zone back arc, *J. geophys. Res.*, **105**, 16 181–16 191.
- Favier, N., Chevrot, S. & Komatitsch, D., 2004. Near-field influences on shear wave splitting and traveltime sensitivity kernels, *Geophys. J. Int.*, **156**, 467–482.
- Karato, S., Jung, H., Katayama, I. & Skemer, P., 2008. Geodynamic significance of seismic anisotropy of the upper mantle: new insights from laboratory studies, *Annu. Rev. Earth planet. Sci.*, **36**, 59–95.
- Kummerow, J. & Kind, R., 2006. Shear wave splitting in the Eastern Alps observed at the TRANSALP network, *Tectonophysics*, **414**, 177–195.
- Lev, E., Long, M.D. & Van Der Hilst, R.D., 2006. Seismic anisotropy in eastern Tibet from shear wave splitting reveals changes in lithospheric deformation, *Earth planet. Sci. Lett.*, **251**, 293–304.
- Levin, V., Menke, W. & Park, J., 1999. Shear wave splitting in the Appalachians and the Urals: a case for multilayered anisotropy, *J. geophys. Res.*, **104**, 17 975–17 993.
- Levin, V., Droznin, D., Park, J. & Gordeev, E., 2004. Detailed mapping of seismic anisotropy with local shear waves in southeastern Kamchatka, *Geophys. J. Int.*, **158**, 1009–1023.
- Li, A., Forsyth, D.W. & Fischer, K.M., 2003. Shear velocity structure and azimuthal anisotropy beneath eastern North America from Rayleigh wave inversion, *J. geophys. Res.*, **108**, doi:10.1029.2002JB002259.
- Liu, H., Davis, P.M. & Gao, S., 1995. SKS splitting beneath southern California, *Geophys. Res. Lett.*, **22**, 767–770.
- Long, M.D. & Silver, P.G., 2009. Shear wave splitting and mantle anisotropy: measurements, interpretations, and new directions, *Surv. Geophys.*, **30**, 407–461.
- Long, M.D. & Van Der Hilst, R.D., 2005a. Estimating shear wave splitting parameters from broadband recordings in Japan: a comparison of three methods, *Bull. seism. Soc. Am.*, **95**, 1346–1358.
- Long, M.D. & Van Der Hilst, R.D., 2005b. Upper mantle anisotropy beneath Japan from shear wave splitting, *Phys. Earth planet. Inter.*, **151**, 206–222.
- Long, M.D., de Hoop, M.V. & Van Der Hilst, R.D., 2008. Wave-equation shear wave splitting tomography, *Geophys. J. Int.*, **172**, 311–330.
- Marone, F. & Romanowicz, B., 2007. The depth distribution of azimuthal anisotropy in the continental upper mantle, *Nature*, **447**, 198–201.
- Menke, W. & Levin, V., 2003. The cross-convolution method for interpreting SKS splitting observations, with application to one and two-layer anisotropic earth models, *Geophys. J. Int.*, **154**, 379–392.
- Montagner, J.-P., Griot-Pommerehne, D.A. & Lavé, J., 2000. How to relate body wave and surface wave anisotropy?, *J. geophys. Res.*, **105**, 19 015–19 027.
- Monteiller, V. & Chevrot, S., 2010. How to make robust splitting measurements for single-station analysis and three-dimensional imaging of seismic anisotropy, *Geophys. J. Int.*, **182**, 311–328.
- Özalaybey, S. & Savage, M.K., 1994. Double layer anisotropy resolved from S phases, *Geophys. J. Int.*, **117**, 653–664.
- Özalaybey, S. & Savage, M.K., 1995. Shear wave splitting beneath western United States in relation to plate tectonics, *J. geophys. Res.*, **100**, 18 135–18 149.
- Panning, M.P. & Nolet, G., 2008. Surface wave tomography for azimuthal anisotropy in a strongly reduced parameter space, *Geophys. J. Int.*, **174**, 629–648.

- Rümpker, G. & Silver, P.G., 1998. Apparent shear wave splitting parameters in the presence of vertically varying anisotropy, *Geophys. J. Int.*, **135**, 790–800.
- Ryberg, T., Rümpker, G., Haberland, C., Stromeyer, D. & Weber, M., 2005. Simultaneous inversion of shear wave splitting observations from seismic arrays, *J. geophys. Res.*, **110**, B03301, doi:10.1029/2004GB003303.
- Saltzer, R.L., Gaherty, J. & Jordan, T.H., 2000. How are vertical shear wave splitting measurements affected by variations in the orientation of azimuthal anisotropy with depth? *Geophys. J. Int.*, **141**, 374–390.
- Savage, M.K., 1999. Seismic anisotropy and mantle deformation: what have we learned from shear wave splitting? *Rev. Geophys.*, **37**, 65–106.
- Savage, M.K. & Silver, P.G., 1993. Mantle deformation and tectonics: constraints from seismic anisotropy in the western United States, *Phys. Earth planet. Inter.*, **78**, 207–227.
- Sieminski, A., Liu, Q., Trampert, J. & Tromp, J., 2007. Finite-frequency sensitivity of body waves to anisotropy based upon adjoint methods. *Geophys. J. Int.*, **171**, 368–389.
- Sieminski, A., Paulssen, H., Trampert, J. & Tromp, J., 2008. Finite-frequency SKS splitting: measurement and sensitivity kernels, *Bull. seism. Soc. Am.*, **98**, 1797–1810.
- Silver, P.G. & Chan, W.W., 1991. Shear wave splitting and subcontinental mantle deformation, *J. Geophys. Res.*, **96**, 16,429–16,454.
- Silver, P.G. & Savage, M.K., 1994. The interpretation of shear-wave splitting parameters in the presence of two anisotropic layers, *Geophys. J. Int.*, **119**, 949–963.
- Simons, F.J., Van Der Hilst, R.D., Montagner, J.-P. & Zielhuis, A., 2002. Multimode Rayleigh wave inversion for heterogeneity and azimuthal anisotropy of the Australian upper mantle, *Geophys. J. Int.*, **151**, 738–754.
- Snyder, D. & Bruneton, M., 2007. Seismic anisotropy of the Slave craton, NW Canada, from joint interpretation of SKS and Rayleigh waves, *Geophys. J. Int.*, **169**, 170–188.
- Vecsey, L., Plomerová, J. & Babuska, V., 2008. Shear-wave splitting measurements: problems and solutions, *Tectonophysics*, **462**, 178–196.
- Vinnik, L., Kind, R., Kosarev, G.L. & Makeyeva, L., 1989. Azimuthal anisotropy in the lithosphere from observations of long-period S-waves, *Geophys. J. Int.*, **99**, 549–559.
- Walker, K.T., Bokelmann, G.H.R. & Klemperer, S.L., 2001. Shear-wave splitting to test mantle deformation models around Hawaii, *Geophys. Res. Lett.*, **28**, 4319–4322.
- Wolfe, C.J. & Silver, P.G., 1998. Seismic anisotropy of oceanic upper mantle: shear-wave splitting observations and methodologies, *J. geophys. Res.*, **103**, 749–771.
- Wüstefeld, A. & Bokelmann, G., 2007. Null detection in shear-wave splitting measurements, *Bull. seism. Soc. Am.*, **97**, 1204–1211.
- Wüstefeld, A., Bokelmann, G., Barruol, G. & Montagner, J.-P., 2009. Identifying global seismic anisotropy patterns by correlating shear-wave splitting and surface-wave data, *Phys. Earth planet. Inter.*, **176**, 198–212.
- Yuan, H. & Romanowicz, B., 2010. Lithospheric layering in the North American craton, *Nature*, **466**, 1063–1068.